IJISEM
INTERNATIONAL JOURNAL OF INNOVATIONS IN SCIENCE ENGINEERING AND MANAGEMENT

International Journal of Innovations In Science Engineering And Management

OPEN ACCESS

Volume: 4

Issue: 1

Month: January

Year: 2025

ISSN: 2583-7117

Published: 25.01.2025

Citation:

Usmani Yasir Arquam, Dr. Shivendra Singh, Dr. B. Suresh "Enhance the heat transfer in the solar air heater by attaching the fins in the absorber plate" International Journal of Innovations In Science Engineering And Management, vol. 4, no. 1, 2025, pp. 96–105.

DOI:

10.69968/ijisem.2025v4i196-105

Enhance The Heat Transfer in The Solar Air Heater by Attaching the Fins in The Absorber Plate

Usmani Yasir Arquam[1], Shivendra Singh[2], Dr. B. Suresh[3]
[1]Research Scholar, Department of Mechanical Engineering, Corporate Institute Of Science & Technology, Bhopal
2Asst. Prof., Department of Mechanical Engineering, Corporate Institute Of Science & Technology, Bhopal
[3]Prof. & HOD, Department of Mechanical Engineering, Corporate Institute Of Science & Technology, Bhopal

Abstract
Due to the high cost of solar air heating systems, performed a parametric analysis to find ways to improve their efficiency. Solar air heating systems with ribs, a novel design, are the subject of the research. Carry out a numerical investigation of a "solar air heater" in "ANSYS Fluent" using "computational fluid dynamics" (CFD) for this work. Enhanced the absorber plate by modifying the pitch and adding more ribs. In order to get the best possible outcome, it was necessary to evaluate the outlet temperature, air temperature inside the duct, friction factor, and heat transfer rate. Case 4, having a maximum outlet temperature, air temperature inside the duct, friction factor, and heat transfer rate with increment of 4.75 %, 1.11%, 35.5%, and 5.52% from case 1 respectively.

Keywords; Ribs or obstacle, Heat transfer rate, Duct, Solar air heater, Absorber plate

INTRODUCTION

The transport of heat is possible via any substance that contains atoms and molecules. A wide range of movements are always occurring among atoms. As a result of atomic and molecular mobility, all matter has thermal energy. There will be more heat energy when there is greater molecular mobility [1], [2]. But when speak about heat transfer, what really mean is the movement of heat from an object with a high temperature to one with a low temperature [3], [4].

"Heat transfer" refers to a subfield of thermal engineering that focusses on the study of heat and its generation, consumption, transformation, and transport across various physical systems. Several processes may be used to transmit heat, including conduction, convection, radiation, and energy transfer via phase shifts [5]. As an additional means of heat transmission, engineers think about the advectional mass transfer of different chemical species, which may be hot or cold. Although these processes are unique, they often coexist in the same system [6], [7].

Heat conduction, also called diffusion, is the microscopic transfer of kinetic energy from one system to another across interfaces, whether those interfaces are molecules or quasiparticles such as lattice waves [8]. When the temperature of an item is slightly more than or equal to the ambient temperature or the temperature of any other body with which it comes into thermal contact, consider that the object has attained thermal equilibrium [9], [10]. According to the second rule of thermodynamics, this kind of spontaneous heat transfer can never take place in a vacuum; it can only take place between two regions of different temperatures [11].

These collectors consist of metal housings with a dark-coloured absorber plate above a transparent protective glass cover [12]. Conventionally, insulation is applied to the sides and bottom of the collector in order to reduce heat dissipation to other sections of the collector. The absorber plate is hit by solar radiation as it passes through the transparent glass [13]. The absorber plate acts as a heat transfer medium, allowing hot water or air to be trapped between the glass and plate [14]. Occasionally, these absorber plates are coated with specialised materials specifically formulated to enhance heat absorption and retention characteristics compared to conventional black paint [15]. Typically, these plates are constructed from conductive metals; copper or aluminium are often used.

Research on solar air heaters has demonstrated significant potential in enhancing thermal performance through various design modifications and the incorporation of obstacles. However, there remains a substantial research gap in optimizing these enhancements to maximize the outlet air temperature effectively. While numerous studies have explored different configurations of absorber plates, fin designs, and the placement of obstacles to improve heat transfer rates, there is limited comprehensive analysis on the synergistic effects of combining multiple design modifications. Specifically, the impact of increasing the number and complexity of obstacles within the air flow path to disrupt laminar flow and promote turbulence, thereby enhancing heat transfer, requires further investigation. Additionally, the long-term performance and durability of these modified designs under real-world operating conditions are not well-documented. There is also a need for advanced computational and experimental studies to quantify the exact improvements in thermal efficiency and to establish standardized guidelines for the design and implementation of optimized solar air heaters. Addressing these gaps could lead to more efficient and practical solar air heating systems, contributing significantly to sustainable energy solutions.

RESEARCH METHODOLOGY

Governing equation

The numerical model for simulations is based on the following assumptions: -

- There is a stable regime and the flow is three-dimensional. This is an incompressible, turbulent flow.
- Throughout, the fluid's thermos-physical characteristics are taken for granted,
- Neither radiation nor viscous dissipation is significant.

Equations derived from conservation laws control thermal and mechanical processes. Energy, momentum, and mass conservation rules are all part of this set. The following are the three-dimensional versions of these governing equations:

The continuity equation:

$$\frac{\partial u_i}{\partial x_i} = 0, \quad where\ (i,j = 1,2,3)$$

The momentum equation;

$$\frac{\partial}{\partial x_i}\left(\rho u_i u_j - \tau_{ij}\right) = -\frac{\partial P}{\partial x_i}$$

Stress equation

$$\tau_{ij} = 2\mu S_{ij} - \frac{2}{3}\mu_t \frac{\partial u_k}{\partial x_k}\delta_{ij}$$

Where,

$$S_{ij} = \frac{1}{2}\left(\frac{\partial u_i}{\partial u_j}\frac{\partial u_j}{\partial u_i}\right)$$

$$\delta_{ij} = \begin{cases} 1 \\ 0 \end{cases} \left\langle if \left| \begin{matrix} i = j \\ i \neq j \end{matrix} \right.\right.$$

$$\mu_t = \left(\rho c_\mu K^2/\varepsilon\right)$$

The ernergy equation:

$$\frac{\partial(\rho u_i T)}{\partial x_i} = \frac{\partial}{\partial x_i}\left(\frac{\partial T}{\partial x_i}\frac{(\lambda)}{C_p}\right)$$

Computational model

The dimensions of the virtual absorber are 1.2 m in length, 0.3 m in width, and 0.0 3 m in height. The model is divided into three pieces, as seen in the image: an output channel measuring 0.3 m, a test channel measuring 1.2 m, and an intake channel measuring 0.5 m. An aluminium absorption plate, measuring 0,002 m in thickness, was erected 500 mm from the entry point and fixed to the duct's top wall. The duct areas are precisely measured to be 2 meters long, 0.3 meters wide, and 0.03 meters high. Theoretically, a turbulent convective airflow is supposed to push its way through the intake channel. The absorber is heated by a continuous solar heat flux of 1000 W/m^2. A layer of 0.06-meter glass wool thermal insulation is attached

to the back of the heater to stop heat loss. To further limit heat exchange with the surroundings, the top of the heater is insulated with a 0.125 m thick wooden covering. Additionally, the steady-state turbulent flow of heated air is considered. In order to enhance the performances of solar air heater system considered ribs of rectangular shape of 25 mm and 20 mm, and thickness of 2 mm, with five holes of 6 mm diameter. Arrangement of hole in rectangular perforated are presented in figure 1.

Configuration 1 having 55 ribs with 3 ribs in odd row and 2 ribs in even row. Ribs attached at 30 mm distance at starting of absorber. In odd row, distance between each ribs is 62.5 mm, and even row, distance between each ribs is 62.5 mm. Distance between odd row and even row is 30mm, and between identical rows is 100 mm. Configuration 2 having 60 ribs with 3 ribs in odd row and 2 ribs in even row. In odd row, distance between each ribs is 62.5 mm, and in even row, distance between each ribs is 62.5 mm. Distance between odd row and even row is 47.5 mm, and between identical rows is 95 mm. Configuration 3 having 70 ribs with 4 ribs in odd row and 3 ribs in even row. In odd row, distance between each ribs is 40 mm, and in even row, distance between each ribs is 40 mm. Distance between odd row and even row is 58.5 mm, and between identical rows is 117 mm. Configuration 4 having 84 ribs with 4 ribs in odd row and 3 ribs in even row. In odd row, distance between each ribs is 40 mm, and in even row, distance between each ribs is 40 mm. Distance between odd row and even row is 47.5 mm, and between identical rows is 95 mm.

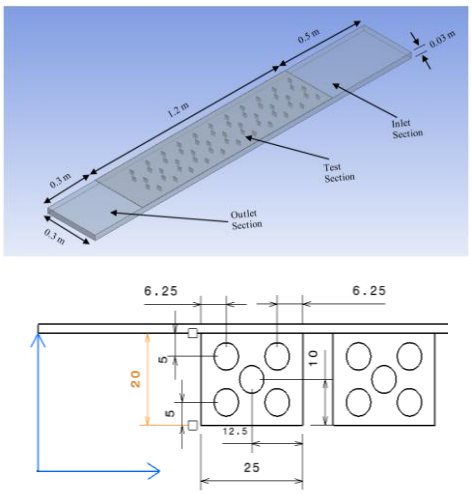

Figure 1 Dimension and all parts representation (dimension in mm)

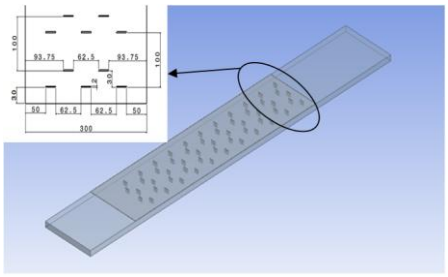

Figure 2 Computational representation of configuration 1 (Rib arrangement and dimension in mm)

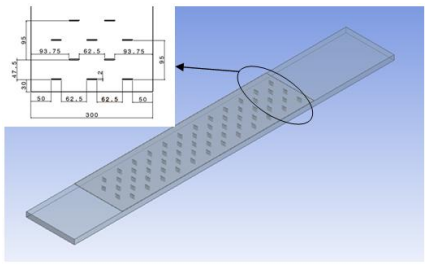

Figure 3 Computational representation of configuration 2 (Rib arrangement and dimension in mm)

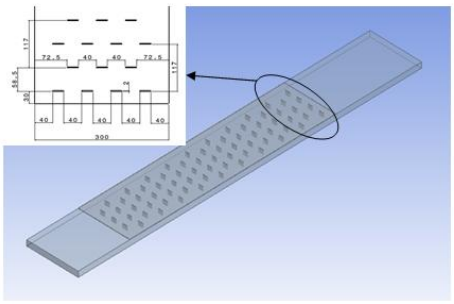

Figure 4 Computational representation of configuration 3 (Rib arrangement and dimension in mm)

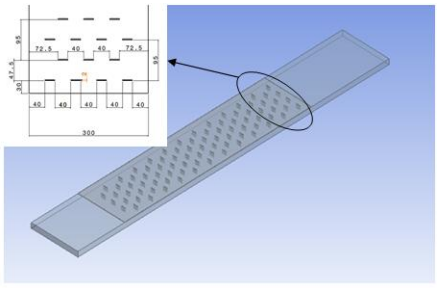

Figure 5 Computational representation of configuration 4 (Rib arrangement and dimension in mm)

Mesh generation

Mesh elements are tetrahedrons with varying sizes for each domain due to the three-dimensional nature of the analysis and the geometric complexity of the computational

domain. All of the solar heater's computational domain, including the ribs, has been mesh-configured in this way. For the obstacle or ribs and the air domain the mesh element size are 0.001 m and 0.008 m respectively. The element's form and side dimensions are same across all solar air heater configurations. Due to mesh generation, element and node are formed in the computational domain, which is mention in table 1.

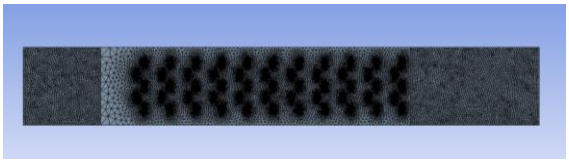

Figure 6 Mesh generation of computational domain

Table 1 Element and Nodes in all configuration

Configuration	Element	Nodes
Configuration 1	2923701	594731
Configuration 2	3184367	647784
Configuration 3	3617456	736668
Configuration 4	4335914	879164

Numerical procedure and boundary condition

The "solar air heater" duct was numerically simulated using ANSYS FLUENT, a "computational fluid dynamics (CFD)" tool. The turbulence phenomenon is represented by the traditional (k-ε) model. In the middle of the control volumes is where the answer you want is computed. Use the Coupled approach to fix the velocity-pressure coupling issue as well. Moreover, a second-order upwind technique and the least-squares cell approach are used to discretise the gradient and pressure variables, respectively. For momentum and energy discretization scheme are second order and turbulent kinetic energy and turbulent dissipation rate, discretization scheme are first order upwind use. The turbulent kinetic energy, turbulent dissipation rate, momentum, pressure, and energy are the five sub-relaxation components. Their corresponding coefficients are set to 0.7, 0.3, 0.7, 0.8, and 0.8. The energy equation's convergence conditions are set to 10-06, whereas the criteria for continuity, velocity, k-equation, and ε-equation are set to 10-04.

In this work 2 computation domain are present, first is fluid, which is flow in the duct, and second is absorber plate with obstacle or rib. Material are select for fluid and absorber plate are air and aluminum respectively. The following table displays the values of the thermo-physical characteristics. Changes in fluid temperature may have an effect on the thermo-physical characteristics of the "heat transfer fluid" (air). A constant mass flow rate of 0.0022 kg/s and a temperature of 27 °C are used to introduce air into the duct. Constant heat flux of 1000 w/m2 are apply to the absorber plate. The outer wall of the duct has insulated. These values will be used throughout this work.

Table 2 Thermo-physical properties

Properties	Density (kg/m3)	Thermal conductivity (W/m.K)	Specific heat (J/kg.K)
Absorber plate (aluminum)	2719	202.4	871

Table 3 Case description

Configuration	Cases	No. of Ribs
Configuration 1	Case 1	55
Configuration 2	Case 2	60
Configuration 3	Case 3	70
Configuration 4	Case 4	84

Validation

A "solar receiver heat exchanger" is a device that uses the sun's rays to generate heat. Even if some of the present solar converters are affordable and simple to use, the problem is coming up with innovative concepts for "solar heating systems" with superior conversion. This is because the air passing through the channel wall has a comparatively low convection coefficient. Present a new idea for a solar air heater that makes use of the finite volume approach and a computational fluid dynamics (CFD) framework. In the top portion, show the framework details. To validate the geometry and boundary condition of the (Salhi et al., 2023)[1],first create the model and simulate with same boundary condition, which is use in (Salhi et al., 2023). After that compare, the simulated result of (Salhi et al., 2023) and result get from present simulation, which is, illustrate in figure 7. For the simulation of ANSYS – fluent software were used. Air is flow at 0.0022 kg/s of mass flow rate with temperature of 27 °C. Aluminum are select for the absorber plate material. For validate the model comparison were conduct in friction factor of both models. The comparison were shows that the difference between both value are small, which is acceptable.

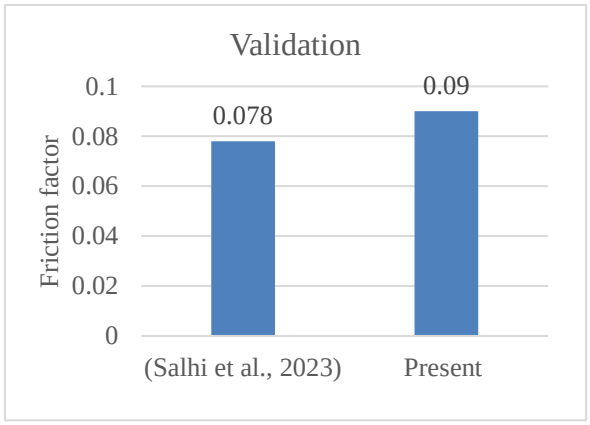

Figure 7 Friction factor comparison for validation

RESULT AND DISCUSSION

Temperature contour

Air is flow with constant mass flow rate of 0.0022 kg/s, at the inlet section there is no change in the behavior of air. When air enter the test section temperature get raise due to constant heat flux of 1000 w/m2 on absorber plate. In all cases, number of obstacle are vary from 55 to 84, so whenever air passes the obstacle temperature get raise. Temperature of air is maximum at the end of the test section when air pass the last row of obstacle. In the outlet section, air get normalize and leave the duct. Create a plane at the middle of the height solar air heater to illustrate the temperature of air, which is show below. For case 1, case 2, case 3, and case 4 value of maximum temperature in middle plane are 312.2 °C, 316.2 °C, 301 °C, and 300 °C respectively.

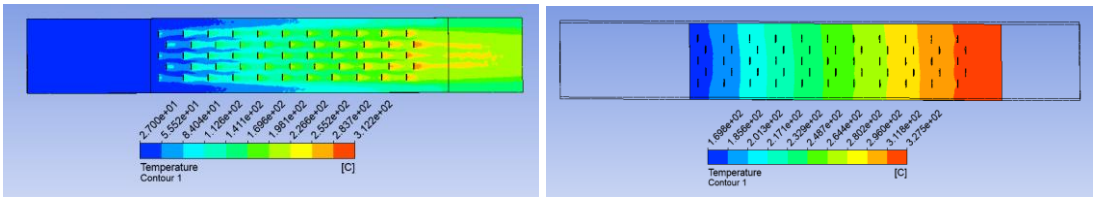

Temperature at middle plane Temperature at absorber plate

Figure 8 Temperature contour in case 1

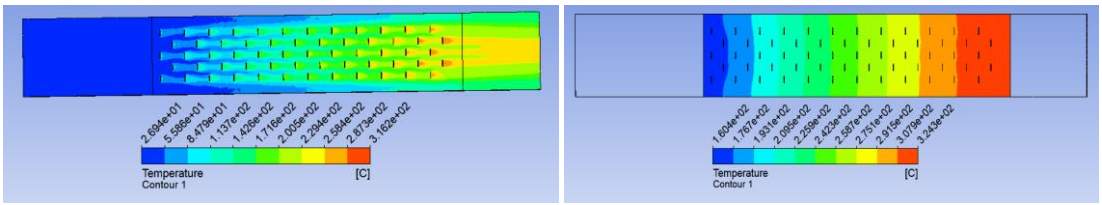

Temperature at middle plane Temperature at absorber plate

Figure 9 Temperature contour in case 2

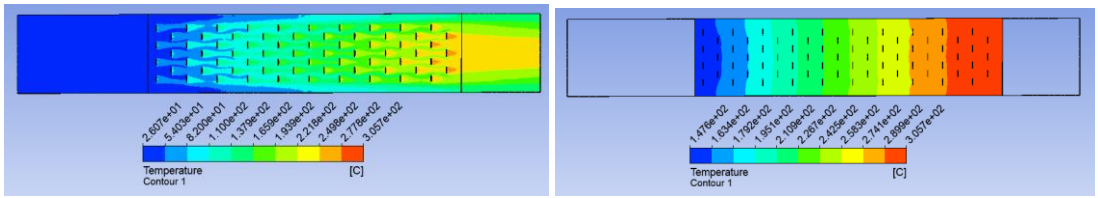

Temperature at middle plane Temperature at absorber plate

Figure 10 Temperature contour in case 3

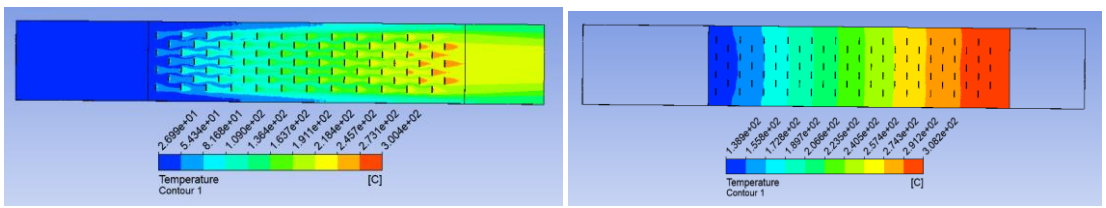

Temperature at middle plane Temperature at absorber plate

Figure 11 Temperature contour in case 4

Turbulent kinetic energy

In fluid dynamics, turbulence is the term used to describe the disorganised motion of different particles in a flowing fluid, which is characterised by unpredictable fluctuations in physical variables, particularly the flow velocity. But turbulence is a thing that makes fluid flow transfer systems more effective mixers. The "turbulent kinetic energy" (TKE), a measure of the force and its strength in the flow field, is often used to quantify the intensity. The turbulent phase may begin at very high amounts of "turbulent kinetic energy" when inertial forces are stronger than viscosity-damping forces. An energy source is necessary to maintain a turbulent flow regime because the turbulence phenomenon is reduced when kinetic energy is converted into internal energy by viscous shear. Because of its importance in characterizing turbulent flows, the "turbulent kinetic energy" (TKE) has to be studied thoroughly in order to assess the intensity distribution of velocity variations.

In addition, the contour map of the TKE could provide light on the thermal events happening in a solar air collector. Case 1 has the lowest TKE, however the data reveal that it grows progressively with increasing rib count. The simulation results show that the ribs are crucial for the turbulent kinetic energy distribution; in particular, reducing the spacing between them increases the fluid's mixing capacity and the numbers that the "turbulent kinetic energy" yields. How much "turbulent kinetic energy" there is depends on where the ribs are.

These results demonstrate, first, that the ribs have a direct effect on the turbulent kinetic energy distribution field of the investigated absorber, and second, that any change in the arrangement of obstacles can alter this field, and hence the flow regime. But, the shear phenomena, caused by the vortices created by the ribs, will grow in severity as the flow gets closer to the ribs. Heat transfer increases with increasing turbulence severity, which is why rough-ribbed solar water heaters are more efficient than smooth ones.

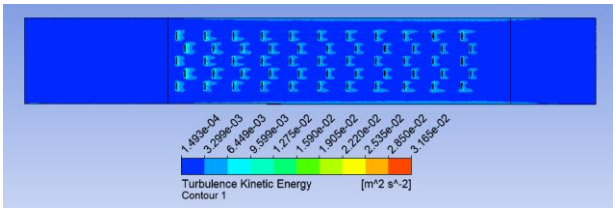

Figure 12 Turbulence kinetic energy of case 1

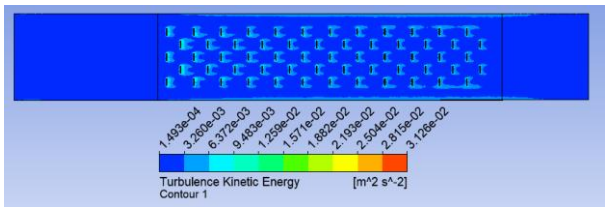

Figure 13 Turbulence kinetic energy of case 2

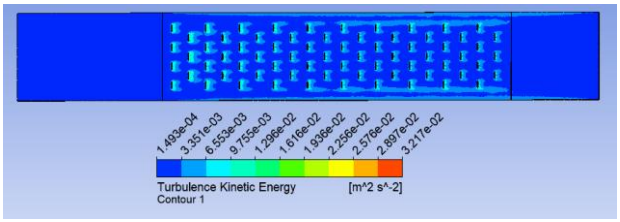

Figure 14 Turbulence kinetic energy of case 3

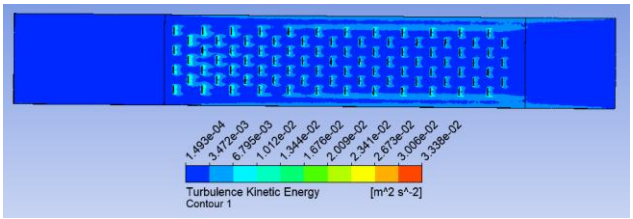

Figure 15 Turbulence kinetic energy of case 4

Pressure contour

In a solar air heater, the behavior of air pressure as it flows through the system is influenced by the presence of ribs or obstacles attached to the absorber plate. At first, the air input to the solar air heater reaches its maximum pressure at the entrance, where it flows at a constant mass flow rate of 0.0022 kg/s. As the air progresses, it collides with the ribs or obstacles, in order to improve heat transmission, they are positioned strategically on the absorber plate. These collisions cause a reduction in pressure while simultaneously increasing both temperature and velocity of the air. The number of ribs or obstacles directly affects the pressure distribution within the solar air heater. An increase in the number of ribs or obstacles causes a more significant reduction in pressure as the air traverses the length of the heater. This is because each rib or obstacle creates additional resistance to airflow, which dissipates energy and thereby reduces pressure. Despite the constant heat flux of 1000 W/m² applied to the absorber plate, the pressure continues to decrease as air moves through the heater. By the time the air reaches the outlet, the pressure drops to zero, indicating that all the energy initially imparted to the air has been dissipated. Therefore, while the introduction of ribs or obstacles enhances the thermal performance by increasing

the air temperature and velocity, it also leads to a pronounced pressure drop along the flow path within the solar air heater.

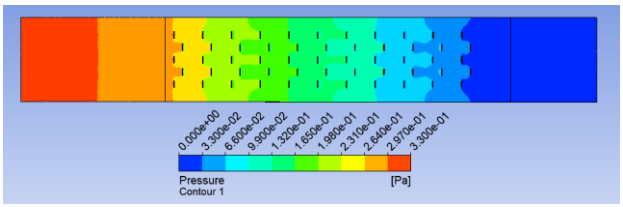

Figure 16 Pressure contour in case 1

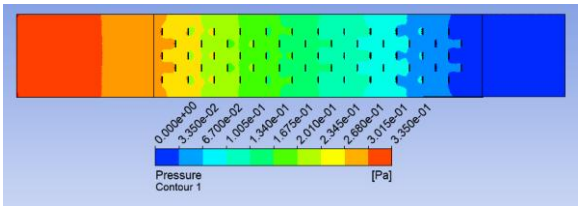

Figure 17 Pressure contour in case 2

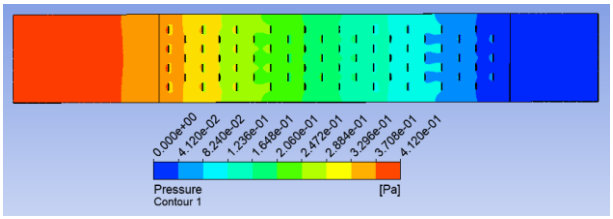

Figure 18 Pressure contour in case 3

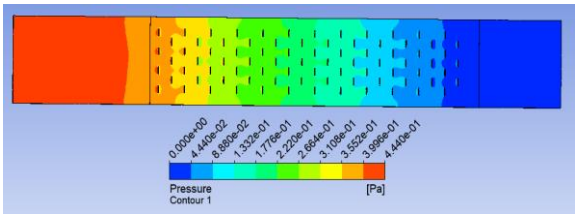

Figure 19 Pressure contour in case 4

Velocity contour

Section of axial velocity distribution across solar air heating channel at mid-duct height is shown in the figure. The computations also maintain a constant mass flow rate of air of 0.0022 kg/s. The statistics show that the air velocity in the duct is increased by the proposed configuration of the absorber plate. Also, the turbulence effect is impacted by the pitch difference between the ribs, which in turn impacts the vortex production phenomena. Adding additional ribs to the channel, or decreasing the pitch of the added ribs, raises the axial velocity of the fluid in the solar air heater's intake and outflow zones. Because they cause axial vortices to form, rib roughness has a direct impact on the flow structure. For all the cases, maximum velocity is between duct wall and ribs. For case 1, case 2, case 3, and case 4 value of the maximum velocity is 0.426 m/s, 0.432 m/s, 0.467 m/s, and 0.496 m/s respectively. Since this results in a higher heat transfer rate, the suggested arrangement is better at transferring heat.

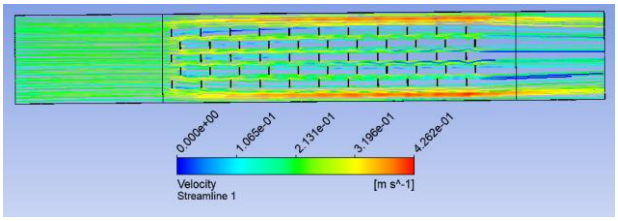

Figure 20 Velocity contour of case 1

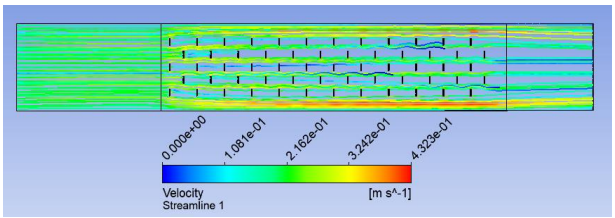

Figure 21 Velocity contour of case 2

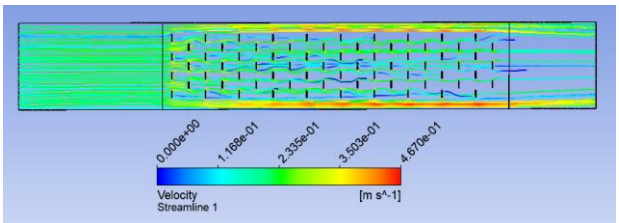

Figure 22 Velocity contour of case 3

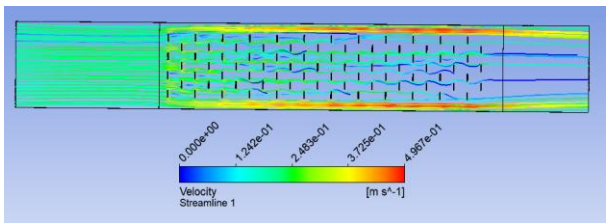

Figure 23 Velocity contour of case 4

Comparison

Solar air heater with 55 ribs on the absorber plate have outlet temperature of air, temperature of air inside duct, and absorber temperature is 192.127 °C, 118.113 °C, and 256.827 °C respectively. Change in the pitch of the ribs and increasing 5 ribs, which indicate the case 2. Outlet temperature of air is increase, and temperature of air inside duct is increase, but in other hand absorber temperature is decreases. Change in the arrangement of the rib because of increasing in the ribs number to the 70, it indicate to case 3. Due to that change in case 3, outlet air temperature is increases, but in other hand temperature inside the duct, and absorber temperature is decrease. In case 4, 84 ribs are present due to that outlet temperature, and temperature inside the duct are increases but absorber temperature are decrease. In case 4, outlet temperature of air, and temperature inside the duct is increases with 4.75 %, and 1.11 % respectively and absorber plate temperature is decrease with 10.11% from the case 1.

Friction factor is a dimension less quantity, which is directly affect by the ribs or obstacle number. Figure show the increases in the as increases in the ribs number friction factor also increases. Fiction factor is maximum at case 4 and minimum at case 1, with 0.122, and 0.09 respectively. Figure illustrate that the heat transfer rate affected by ribs. As increases in the ribs number also increases the heat transfer rate. Case 1 having a minimum heat transfer rate with 365.614 W. case 4 having a maximum heat transfer rate with 385.812 W, which is 5.52 % more than case 1.

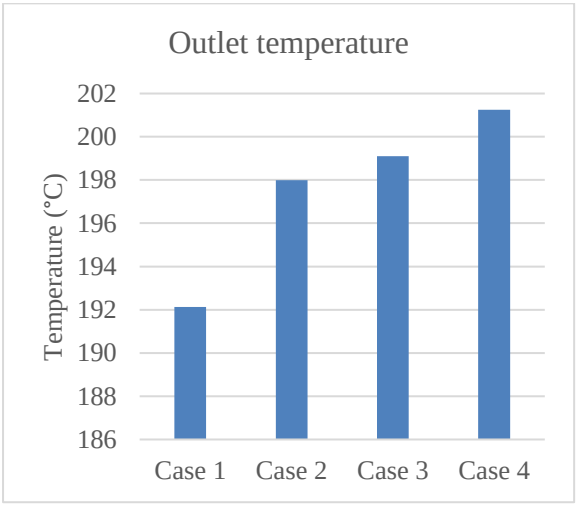

Figure 24 Comparison of outlet air temperature

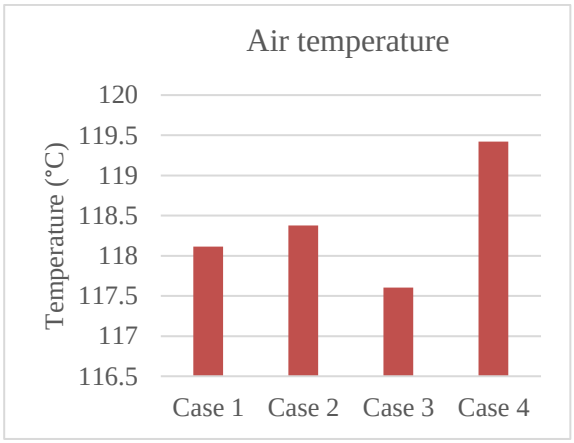

Figure 25 Comparison of air temperature inside the duct

Figure 26 Comparison of absorber plate temperature

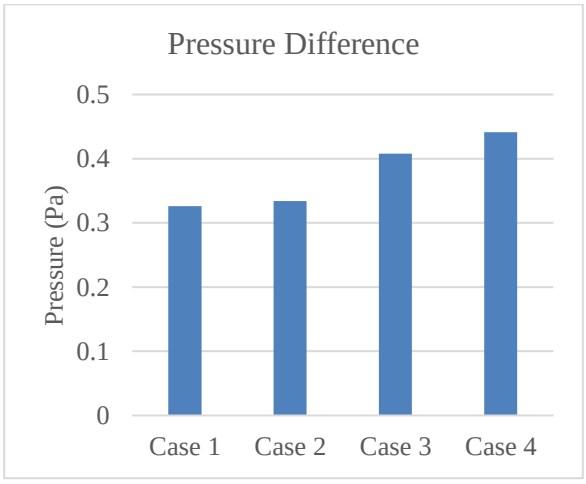

Figure 27 Comparison of pressure difference between inlet and outlet

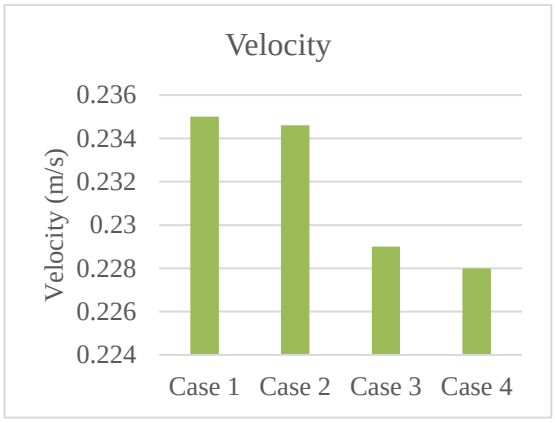

Figure 28 Comparison of velocity at middle of the solar heater height

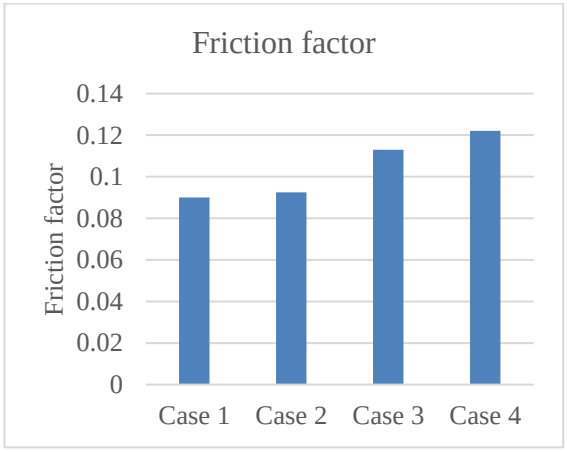

Figure 29 Comparison of friction factor

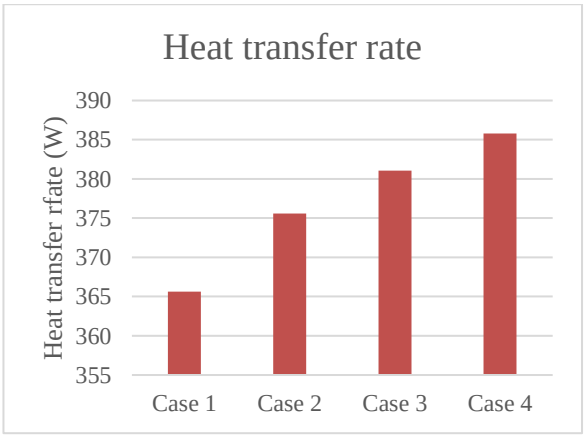

Figure 30 Comparison of heat transfer rate

CONCLUSION

One of the most promising renewable energy sources that everyone is trying to cultivate is solar power. Among its many uses, it is most often seen in farming and manufacturing (solar air heaters, lights). Its demand will likely continue to rise indefinitely due to its status as a clean energy source. This three-dimensional study found the optimal geometric configurations for improving a solar thermal-hydraulic air heater using an absorber plate. The possibility of increasing the plate's thermal efficiency was explored by adding perforated ribs, which increased the contact surface. Presented and evaluated in detail the influence of the channel's and rib's geometrical characteristics on the ideal rib count. Most industries (industrial, agricultural, etc.) are very interested in the research presented here since it helps build one of the most cutting-edge heating systems that use solar energy as a renewable resource. Because of their ubiquitous and varied applications, heating systems have been the primary focus of our research. There is need for improvement in the integration of rib insertion technology, but overall, it can satisfy consumers' demands for solar energy and is quite flexible. Consequently, studies were conducted to include this innovative method into an evaluation of a solar air heater's improvement, and the following conclusions were drawn:

- As the number of ribs rises, heat transfer rate, pressure drop, maximum velocity, temperature within the duct, and air outlet temperature all noticeably rise.
- Increases in the ribs number, reduce the absorber plate temperature.
- Outlet temperature of case 2. Case 3, and case 4 has increases 3.05%, 3.62%, and 4.75 % from case 1 respectively.
- In case 4, air temperature inside the duct is increases 1.11 % from case 1.
- Absorber plate temperature of case 2, case 3, and case 4 is 1.52 %, 7.67%, and 10.11% decreases from case 1 respectively.
- Pressure drop is minimum and maximum for case 1, and case 4 respectively. Pressure drop of case 4 is 35.27% more than from case 1.
- Friction factor of case 2, case 3, and case 4 is 2.78%, 25.5%, and 35.5% increase from case 1 respectively.
- Heat transfer rate of case 2, case 3, and case 4 is 2.73%, 4.22%, and 5.52% increase from case 1 respectively.

REFERENCE

[1] J. E. Salhi *et al.*, “Three-dimensional analysis of a novel solar air heater conception, for an improved heat transfer and energy conversion,” *Energy*

Convers. Manag. X, vol. 19, no. April, p. 100386, 2023, doi: 10.1016/j.ecmx.2023.100386.

[2] L. Yadav, S. Engineering, S. Burman, and L. Yadav, "A Review on Effect of Fluid Flow and Heat Transfer in Various Types of Cavities or Enclosed Object," pp. 80–84, 2023.

[3] I. Sadrehaghighi, "Classical & Numerical Heat Transfer with Case Studies," no. June, p. 14, 2021.

[4] R. Khare, D. Tyagi, I. In, S. Engineering, and R. Khare, "Examine the Heat Transfer Characteristics in Car Radiator Utilizing the Water / Anti- Freezing and Al 2 O 3 / Cuo / Tio 2 Based Nanofluid as Coolant," pp. 17–30, 2025, doi: 10.69968/ijisem.2025v4i117-30.

[5] A. Khanlari *et al.*, "Experimental and numerical study of the effect of integrating plus-shaped perforated baffles to solar air collector in drying application," *Renew. Energy*, vol. 145, pp. 1677–1692, 2020, doi: 10.1016/j.renene.2019.07.076.

[6] M. T. Baissi, A. Brima, K. Aoues, R. Khanniche, and N. Moummi, "Thermal behavior in a solar air heater channel roughened with delta-shaped vortex generators," *Appl. Therm. Eng.*, vol. 165, no. August 2018, p. 113563, 2020, doi: 10.1016/j.applthermaleng.2019.03.134.

[7] A. Raj, S. Singh, and B. Suresh, "Enhanced the solidification of the phase change material in the horizontal latent heat thermal energy storage by using rectangular plate and circular disc plate fins by using CFD," pp. 89–96, 2023.

[8] P. G. Kumar, D. Sakthivadivel, K. Balaji, M. Salman, and S. C. Kim, "Performance enhancement of a double-pass solar air heater with a shot-blasted absorber plate and winglets," *J. Mech. Sci. Technol.*, vol. 35, no. 6, pp. 2743–2753, 2021, doi: 10.1007/s12206-021-0544-x.

[9] S. Touili, A. Alami Merrouni, Y. El Hassouani, A. illah Amrani, and S. Rachidi, "Analysis of the yield and production cost of large-scale electrolytic hydrogen from different solar technologies and under several Moroccan climate zones," *Int. J. Hydrogen Energy*, vol. 45, no. 51, pp. 26785–26799, 2020, doi: 10.1016/j.ijhydene.2020.07.118.

[10] A. Basit, S. Singh, and B. Suresh, "Enhancement the thermal characteristics of PCM By using Various Fin Configurations on the Inner Tube Surface of a Shell and Tube Latent Heat Thermal Energy Storage Unit," pp. 22–31, 2024.

[11] R. kumar *et al.*, "Impact of artificial roughness variation on heat transfer and friction characteristics of solar air heating system," *Alexandria Eng. J.*, vol. 61, no. 1, pp. 481–491, 2022, doi: 10.1016/j.aej.2021.06.031.

[12] P. T. Saravanakumar, D. Somasundaram, and M. M. Matheswaran, "Exergetic investigation and optimization of arc shaped rib roughened solar air heater integrated with fins and baffles," *Appl. Therm. Eng.*, vol. 175, no. November 2019, p. 115316, 2020, doi: 10.1016/j.applthermaleng.2020.115316.

[13] H. Hassan, M. S. Yousef, and S. Abo-Elfadl, "Energy, exergy, economic and environmental assessment of double pass V-corrugated-perforated finned solar air heater at different air mass ratios," *Sustain. Energy Technol. Assessments*, vol. 43, no. December 2020, p. 100936, 2021, doi: 10.1016/j.seta.2020.100936.

[14] A. Khanlari, A. Sözen, F. Afshari, C. Şirin, A. D. Tuncer, and A. Gungor, "Drying municipal sewage sludge with v-groove triple-pass and quadruple-pass solar air heaters along with testing of a solar absorber drying chamber," *Sci. Total Environ.*, vol. 709, 2020, doi: 10.1016/j.scitotenv.2019.136198.

[15] P. Ganesh Kumar, K. Balaji, D. Sakthivadivel, V. S. Vigneswaran, R. Velraj, and S. C. Kim, "Enhancement of heat transfer in a combined solar air heating and water heater system," *Energy*, vol. 221, p. 119805, 2021, doi: 10.1016/j.energy.2021.119805.